Applied problems of nonlinear oscillation and wave theory

Official English translation https://doi.org/10.18500/0869-6632-2019-27-4-71-84

Dynamics and advection in a vortex parquet

A. M. Filimonova

Southern Federal University
105/42, Bolshaya Sadovaya str., Rostov-on-Don 344006, Russia
E-mail: afilimonova@sfedu.ru
Received 26.05.2019, accepted for publication 19.06.2019

Issue. The article is devoted to a numerical study of the dynamics and advection in a vortex parquet. A vortex structure, consisting of vortex patches on the entire plane, is considered. The mathematical model is formulated as a system of two partial differential equations in terms of vorticity and stream function. The dynamics of the vortex structures is considered in a rectangular area under the assumption that periodic boundary conditions are imposed on the stream function. **Investigation methods.** The non-stationary problem is solved by the meshless vortex-in-cell method, based on the vorticity field approximation by its values in liquid particles and stream function expansion in the Fourier series cut. **Results.** Vortex structure consisting of four patches with different directions is investigated. The results of a numerical study of the dynamics and interaction of the structure are presented. The influence of the patch radius and the relative position of positively and negatively directed patches on the processes of interaction and mixing is studied. The obtained results correspond to the following possible scenarios: the initial configuration does not change over time; the initial configuration forms a new structure, which is maintained for longer times; the initial configuration returns to its initial state after a certain period of time. The processes of mass transfer of vorticity by liquid particles on a plane were calculated and analyzed. The results of a numerical analysis of the particles dynamics and trajectories on the entire plane and the field of local Lyapunov exponents are presented.

Key words: ideal fluid, meshless methods, vortex structures in liquids, vortex parquet.

Reference: Filimonova A.M. Dynamics and advection in a vortex parquet. *Izvestiya VUZ. Applied Nonlinear Dynamics*, 2019, vol. 27, no. 4, pp. 71–84. https://doi.org/10.18500/0869-6632-2019-27-4-71-84

Introduction

Unsteady vortex structures play a significant role in the atmosphere, geophysical processes, mass transfer, the emergence and development of turbulence. Such configurations may consist, for example, of several distributed vortex patches with different sizes, intensities and rotation directions. The study of the qualitative change in such structures over time allows us to study the intensity and direction of mass transfer, fluid dynamics, structural stability of a given configuration. All these issues are not thoroughly studied yet. In order to do so it is necessary to evaluate the qualitative and quantitative characteristics of vortex configurations at various points in time, i.e. it requires the development of special numerical algorithms.

Various vortex methods [1–3] are widely used to solve non-stationary problems of fluid dynamics. In this paper, for the numerical analysis of the dynamics and interaction of vortex structures, the vortex-in-cell method proposed and developed by [4] and [5] is used. This method is based on solving equations determining the distribution of the vorticity field. The velocity field and all other characteristics of the fluid flow are calculated for the reconstructed vorticity field. The described numerical scheme serves as a necessary computational tool for analyzing the dynamics of the vortex configuration, its qualitative and quantitative changes over time, as well as the characteristics of passive mass transfer.

In this paper, I study the dynamics and advection in a vortex parquet. To study the processes of interaction and mixing, we consider a structure consisting of symmetrically located vortex patches of different rotation directions that occupies the entire plane. The centers of the patches are located in the nodes of the evenly spaced grid. The correlation between the radius and the relative position of patches of different directions on the one hand and the dynamics and formation of vortex structures on the other was studied. To evaluate the processes of interaction and mixing, I studied the field of local Lyapunov exponents, which are a modern tool for the numerical analysis of such processes.

Kolmogorov theory of flows [6] is widely used to numerically study the dynamics of vortex parquet, including those on the infinite plane [7], as well as ABC flows [8] and CABC flows [9]. An ABC flow is a three-dimensional stationary flow of an ideal incompressible fluid for which the condition of collinearity of the velocity field to its rotor is satisfied (Beltrami condition). This flow was first studied by V. I. Arnold in 1965. The CABC flow is analogous to the ABC flow for a compressible fluid. In the cases described above, the model solution is investigated. The problem of the dynamics of vortex parquet and its solution in complete equations are still poorly studied.

There is a possibility of the formation of quasistationary structures in an ideal fluid. Those structures were observed in model problems, which is reflected in the works [9–11]. In particular, a structure was discovered that ensured the formation of the so-called stochastic web on the plane. The presence of webs determines the unevenness of the passive transfer of liquid particles on the plane and the special properties of mass transfer.

The article is structured as follows: the mathematical formulation of the problem of two-dimensional vortex dynamics is given in the first section, the methods for studying the dynamics of vortex structures numerically are briefly described in the second section. The third section is devoted to the analysis of the results of computational experiments. The advection of particles in a vortex parquet is analyzed in the fourth section. In conclusion, the results are summarized.

1. Mathematical formulation of the problem

The plane flows of an inviscid incompressible fluid are considered. Mathematically, this problem can be defined by a system of two partial differential equations regarding the vorticity of $\omega = \omega(x, y)$ and the stream function $\psi = \psi(x, y)$:

$$\begin{cases} \dfrac{D\,\omega}{D\,t} \equiv \omega_t + \psi_y\,\omega_x - \psi_x\,\omega_y = 0, \\ -\triangle\psi = \omega, \end{cases} \tag{1}$$

where D/Dt is the material time derivative, t, x, y are the spatial variables by which the differentiation is performed, $\triangle$ is the Laplace operator. The system (1) is called the Euler equations for the dynamics of an inviscid incompressible fluid in terms of vorticity and stream function. The first equation of the system (1) defines the passive transfer of absolute vorticity by liquid particles. The second equation of the system (1) relates the vorticity of ω and the stream function ψ. The following formulas express the fluid velocity field $\mathbf{v} = (v_1, v_2)$ through the stream function:

$$v_1 = \psi_y(x, y), \quad v_2 = -\psi_x(x, y). \tag{2}$$

The dynamics of fluid particles is defined by the following system of equations:

$$\begin{cases} \dot{x}_i = v_1 = \psi_y(x_i, y_i), \\ \dot{y}_i = v_2 = -\psi_x(x_i, y_i), \end{cases} \tag{3}$$

where the dot denotes time differentiation.

At the initial moment of time, the distribution of vorticity in the area is defined by the following condition: $\omega|_{t=0} = \omega_0(x, y)$.

This problem is solved under the assumption that the boundary conditions, periodic in both spatial variables, are imposed on the stream function ψ and its derivative:

$$\psi|_{x=-a} = \psi|_{x=a}, \quad \psi|_{y=-b} = \psi|_{y=b}, \quad \psi'_x|_{x=-a} = \psi'_x|_{x_x=a}, \quad \psi'_y|_{y=-b} = \psi'_y|_{y=b}. \tag{4}$$

Such boundary conditions are often used in modeling fluid flows on the entire plane. These conditions properly reflect the considered in this work problem of studying the vortex configuration consisting of vortex patches with centers at the nodes of an evenly spaced rectangular grid.

An infinite configuration is considered, but the rectangle $D = \{-a < x < a, -b < y < b\}$ is the computational domain for solving the system (1). Thus, a section of the vortex parquet is considered, and the dynamics on the entire remaining plane is repeated due to periodic boundary conditions.

In the computational domain, I considered symmetric vortex configurations consisting of four identical vortex patches which centers are located at nodes of an evenly spaced grid. At the initial time, the vorticity distribution was set according to the Gaussian distribution:

$$\omega_0(x, y) = \begin{cases} \dfrac{1}{\sqrt{2\pi}} e^{-\frac{(x\mp\alpha)^2+(y\pm\beta)^2}{2}}, & (x \mp \alpha)^2 + (y \pm \beta)^2 \leq R^2, \\ -\dfrac{1}{\sqrt{2\pi}} e^{-\frac{(x\pm\alpha)^2+(y\pm\beta)^2}{2}}, & (x \pm \alpha)^2 + (y \pm \beta)^2 \leq R^2, \\ 0, & (x \pm \alpha)^2 + (y \pm \beta)^2 > R^2, \\ 0, & (x \mp \alpha)^2 + (y \pm \beta)^2 > R^2, \end{cases} \tag{5}$$

where $(\pm\alpha, \pm\beta)$, $(\mp\alpha, \pm\beta)$ are coordinates of the centers of the four vortex patches, R is a radius of the vortex patches.

For the solution of the second equation of the system (1) to exist, it is necessary that the integral of the total vorticity in the computational domain be equal to zero. This condition is satisfied due to the initial vorticity distribution defined by the law (5).

2. Methods for the numerical analysis of the dynamics of plane vortex configurations

This section presents an algorithm for calculating and analyzing the dynamics and interaction of distributed vortex configurations on a plane. The developed algorithm allows calculating the dynamics of an inviscid incompressible fluid using a variant of the vortex-in-cell method, constructing a phase portrait of the fluid velocity field at each time step, and also studying the numerical characteristics of mass transfer in the area by calculating the field of local Lyapunov exponents.

2.1. Calculation of fluid dynamics. For the numerical solution of the problem (1)-(4), a variant of the meshless vortex-in-cell method is used, which was proposed and described in detail in [4,12,13].

In this paper, an algorithm based on the following procedures is implemented:

1. At the initial moment of time, the vorticity field is set discretely by the values in N liquid particles: $\omega(x_i, y_i)|_{t=0} = \omega_i$. The value of ω_i is stored in the $i-$ liquid particle over time, which is derived from the first equation of the system (1).

2. The stream function ψ at each time step is approximated by a segment of the Fourier series:

$$\psi \approx \sum_{i=1}^{k_x} \sum_{j=1}^{k_y} \psi_{ij}\, g_i(x)\, h_j(y),$$

where $g_i(x)$, $h_j(y)$ are trigonometric basis functions satisfying periodic boundary conditions, k_x, k_y are the number of expansion terms in x and y, respectively, ψ_{ij} are unknown coefficients that are calculated at each moment in time by the Bubnov-Galerkin projection method.
3. The vorticity field $\omega(x, y)$ is approximated at each time step. To do this, the area D is divided into $N_{box} = n_x \times n_y$ rectangular cells, in each of those the vorticity field $\omega(x, y)$ is approximated by third degree polynomials with their polynomial coefficients being calculated by the method of least squares.
4. The dynamics of liquid particles is defined by a system of ordinary differential equations:

$$\dot{x} = v_1(x, y), \quad \dot{y} = v_2(x, y).$$

This system is solved by the pseudo-symplectic Runge-Kutta method accurate to order 3 (6), see [14]. The choice of this integration method is justified in [13].

2.2. Calculation of the field of local Lyapunov exponents. The Lyapunov exponents make it possible to estimate how infinitely close the trajectories are moving away from each other in the phase space over time. Studying their spectrum makes it possible to determine the type of dynamics and its dependence on the magnitude of certain system parameters. Since fluid flows are considered at finite time intervals, local Lyapunov exponents (LLE) are studied. The magnitude of the LLE depends on the initial coordinates of the particles of the entire vortex configuration and the integration time. Following the works of [15, 16], I describe the concept of LLE and the algorithm for their calculation.

Let $\mathbf{u}(t) = (x(t), y(t))$ be the coordinates of a liquid particle on a plane which initial position is defined by the condition: $\mathbf{u_0} = (x(t_0), y(t_0))$. Each particle is transported over time by a fluid field of the form: $\mathbf{v} = (v^{(x)}, v^{(y)})$. This process is defined by the following Cauchy problem:

$$\dot{\mathbf{u}} = \mathbf{v}(t, \mathbf{u}), \quad \mathbf{u}(t_0) = \mathbf{u_0}. \tag{6}$$

The problem (6) is a shift along the trajectory over a certain period of time T, which can be defined by the map: $u(t_0 + T) = \phi_{t_0}^{t_0+T}(u_0)$. The initial perturbation at time T will be defined as followed:

$$\delta\mathbf{u}(T) = \phi_{t_0}^{t_0+T}(u_0 + \delta\mathbf{u}(t_0)) - \phi_{t_0}^{t_0+T}(\mathbf{u_0}) = \frac{d\phi_{t_0}^{t_0+T}(u_0)}{d\mathbf{u}}\delta\mathbf{u}(t_0) + O(\| \delta\mathbf{u}(t_0)^2 \|), \tag{7}$$

where $\frac{d\phi_{t_0}^{t_0+T}(u_0)}{d\mathbf{u}}$ is the tensor of the displacement gradient along the trajectory. Using the Cauchy-Green strain tensor L for a finite instant of time T, we obtain:

$$L = \frac{d\phi_{t_0}^{t_0+T}(u_0)^*}{d\mathbf{u}} \frac{d\phi_{t_0}^{t_0+T}(u_0)}{d\mathbf{u}}, \tag{8}$$

where an asterisk denotes a conjugation. Then the perturbation value (7) can be estimated by the norm:

$$\| \delta\mathbf{u}(T) \| = \sqrt{\left\langle \frac{d\phi_{t_0}^{t_0+T}(u_0)^*}{d\mathbf{u}}\delta\mathbf{u}(t_0), \frac{d\phi_{t_0}^{t_0+T}(u_0)}{d\mathbf{u}}\delta\mathbf{u}(t_0) \right\rangle} = \sqrt{\langle \delta\mathbf{u}(t_0), L\delta\mathbf{u}(t_0) \rangle}. \tag{9}$$

Infinitely close trajectories will most likely recede along the direction of the eigenvector corresponding to the maximum eigenvalue $\lambda_{max}(L)$ of the operator L:

$$\max_{\delta\mathbf{u}(t_0)} \| \delta\mathbf{u}(T) \| = \sqrt{\lambda_{max}(L)} \| \delta\mathbf{u}(t_0) \|, \tag{10}$$

where $\delta\mathbf{u}(t_0)$ is aligned with the eigenvector corresponding to the eigenvalue $\lambda_{max}(L)$. At the point $\mathbf{u}(t_0)$ on the time interval T the LLE is defined by the following formula:

$$\sigma_{t_0}^{T}(\mathbf{u}(t_0)) = \frac{1}{|T|} ln \sqrt{\lambda_{max}(L)} \| \delta\mathbf{u}(t_0) \| . \tag{11}$$

It should be noted that it follows from (11) that for $T \to +\infty$:

$$\sigma_{t_0}^{T}(\mathbf{u}(t_0)) \to \mathrm{const} = \max_{\delta\mathbf{u}(t_0)} \| \delta\mathbf{u}(T) \| .$$

In the case when LLE are considered in a certain area of the phase space, we can talk about the LLE field. For numerical construction of the field in the computational domain D at the initial time, points with coordinates $\mathbf{u}_i = (x_i(t_0), y_i(t_0))$ at the nodes of a rectangular grid with steps h_x and $h_y are set$ for x and for y respectively. I will use a four-point pattern, that is, for each point $(x_i(t_0), y_i(t_0))$ adjacent points are defined as followed:

$$\begin{aligned} &\mathbf{u}_i^l = (x_i(t_0) - h_x, y_i(t_0)), \quad \mathbf{u}_i^r = (x_i(t_0) + h_x, y_i(t_0)), \\ &\mathbf{u}_i^d = (x_i(t_0), y_i(t_0) - h_y), \quad \mathbf{u}_i^u = (x_i(t_0), y_i(t_0) + h_y). \end{aligned} \tag{12}$$

The finite difference method is used to approximate the displacement gradient tensor along the trajectory $d\phi_{t_0}^{t_0+T}(\mathbf{u}_0)/d\mathbf{u}$:

$$\frac{d\phi_{t_0}^{t_0+T}(\mathbf{u}_i(t_0))}{d\mathbf{u}} \approx \left| \frac{\phi_{t_0}^{t_0+T}(\mathbf{u}_i^r) - \phi_{t_0}^{t_0+T}(\mathbf{u}_i^l)}{2h_x}, \frac{\phi_{t_0}^{t_0+T}(\mathbf{u}_i^u) - \phi_{t_0}^{t_0+T}(\mathbf{u}_i^d)}{2h_y} \right| . \tag{13}$$

In order to find the value $\phi_{t_0}^{t_0+T}(\mathbf{u}_i(t_0))$ for each particle, it is necessary to solve the Cauchy problem (6) on the time interval $t \in [t_0, t_0 + T]$. The solution to this Cauchy problem is a part of the time step of the vortex-in-cell method. Therefore, the solution of the original problem (1) by the vortex-in-cell method, provided that at the initial moment all the liquid particles are located at the nodes of the evenly spaced grid, allows us to construct an LLE field at each instant of time T. The figures show the constructed LLE fields for further analysis: the darker is the shade of gray, the lower is the LLE value.

3. Dynamics of a system of symmetric vortex patches

Using the vortex-in-cell method, a series of computational experiments were carried out. I studied the interaction, dynamics, and mixing processes in vortex parquet, consisting of pairwise oppositely directed vortex patches of equal radius located at the nodes of an evenly spaced grid. This section presents the results of the experiments. The area of the vortex parquet consisting of four such patches is taken as the computational domain.

At the initial time, for all experiments in (5), the vorticity value was set according to the Gaussian law. Of the four patches, two were taken with a positive vorticity and two with a negative one. This made it possible to take into account the need for the integral to vanish from the total vorticity in this formulation of the problem. The correlation between the radius R and the relative positions of patches of different directions on the one hand and the preservation, destruction or formation of a new vortex structure on the other, as well as on the course of interaction and mixing, was studied.

Computational experiments were carried out in a rectangular region D with sides $a = b = 20$. At the initial moment of time, the field is set with $N = 160,000$ of liquid particles, each having an initial value of vorticity set. To approximate the vorticity field at each time step, the area D is divided into $n_x \times n_y = 35 \times 35$ cells. In the expansion of the stream function $\psi(x, y)$ into the segment of the Fourier series, $k_x \times k_y = 25 \times 25$ of members of the series in x and y, respectively. The time step of the dynamics of liquid particles in most calculations was $\triangle t = 0.005$.

The results of a series of computational experiments are presented below; the top row (figures *a–d*) shows the dynamics of the vortex parquet section at different instants of time, and the bottom row (figures *e–h*) is a LLE field for this configuration at the same time instants. The dynamics reflects the displacement of those liquid particles in the computational domain, which at the initial instant of time constituted the initial vortex configuration. Light gray denotes patches with a total positive vorticity, and black marks those of a total negative vortex.

Visualization of the LLE field shows how infinitely close at the initial moment of time trajectories recede in the phase space over time. Here black color marks the slightest receding (minimum LLE is 0, see the formula (11)), and the lighter the shade of gray, the larger the LLE value and the stronger the receding of particles.

Fig. 1 presents the dynamics of the vortex parquet section (5) for the radius $R = 2.5$. Since this configuration is symmetrical on the entire plane, such a structure does not collapse and practically does not change. It can be assumed that it is sustainable. Each of the patches rotates around its axis at a constant speed, while the entire vortex configuration stands still for the entire calculation interval $t \in [0, 400]$. Each of the patches makes a complete rotation around its axis in $t \approx 10$, that is, for the entire calculation interval, each of the patches has made 40 rotations.

The analysis of the LLE values leads to the conclusion that the passive transport of particles around the initial vortex patches: these particles recede most over time. For $t = 0.2$ (see Fig. 1,*e*), it is clear that the distance between the center of each of the patches and the points close to it is small,

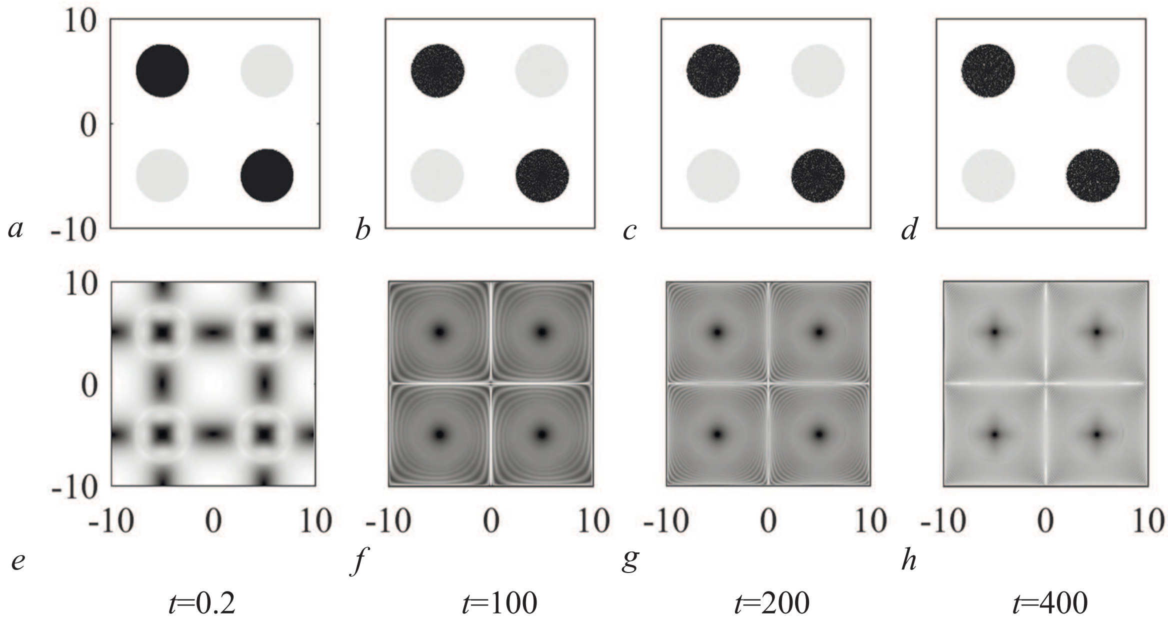

Fig. 1. (*a–d*) – the vorticity distribution on the (x, y) plane and (*e–h*) – the Lyapunov exponents at the specific time t for a vortex configuration of four vortices (5) for $R = 2.5$ and $\alpha = \beta = 5.0$

and the distances between the border points of the patches increase, i.e. these particles move away. At $t = 200$ (see Fig. 1, g), separatrices (white lines) are clearly visible, dividing the computational domain into four equal squares inside which passive particle transport occurs. The centers of the patches and the particles close to them still remain black, that is, these particles do not recede far over time. At $t = 400$ (see Fig. 1, h), the areas inside the squares become even brighter, which indicates mixing.

Transfer to larger distances occurs in a small neighborhood of the separatrices of stationary saddle points of the velocity field on the plane. However, due to the small value of the velocity in these areas, this becomes apparent only at large times.

Fig. 2 presents the results of a computational experiment with the smallest (in the series) radius value $R = 2.0$. In contrast to the previous experiment, this configuration has a displaced center, which makes it possible to obtain a qualitatively different type of vortex parquet dynamics in the computational domain.

At time $t = 10$ (see Fig. 2, a), the four-patch configuration splits into two dipoles, which begin to move in opposite directions. Having reached the boundary of the computational domain in x, the dipoles break up into separate patches again and continue to move in opposite directions along the boundary vertically. At $t = 50$ (see Fig. 2, b) each of the patches reaches the corner of the area and starts moving towards the patch with the total vorticity of the opposite sign. After passing x halfway, the patches again form dipoles, which move to the center of the area. So, by $t \approx 95$ a configuration similar to the initial one is formed. For this calculation, periodic dynamics with a period of $t \approx 95$ are observed. At time $t = 190$ (see fig. 2, c), the configuration returns to its initial state for the second time. Over the entire calculation interval, the configuration makes six complete cycles, with each of the patches making a rotation around its axis in $t \approx 40$.

This is due to the fact that the problem with periodic boundary conditions is being considered, provided that there is only a section of vortex parquet in the computational domain, the same configuration with the same dynamics is located outside the boundaries of this area, i.e., reaching the boundary

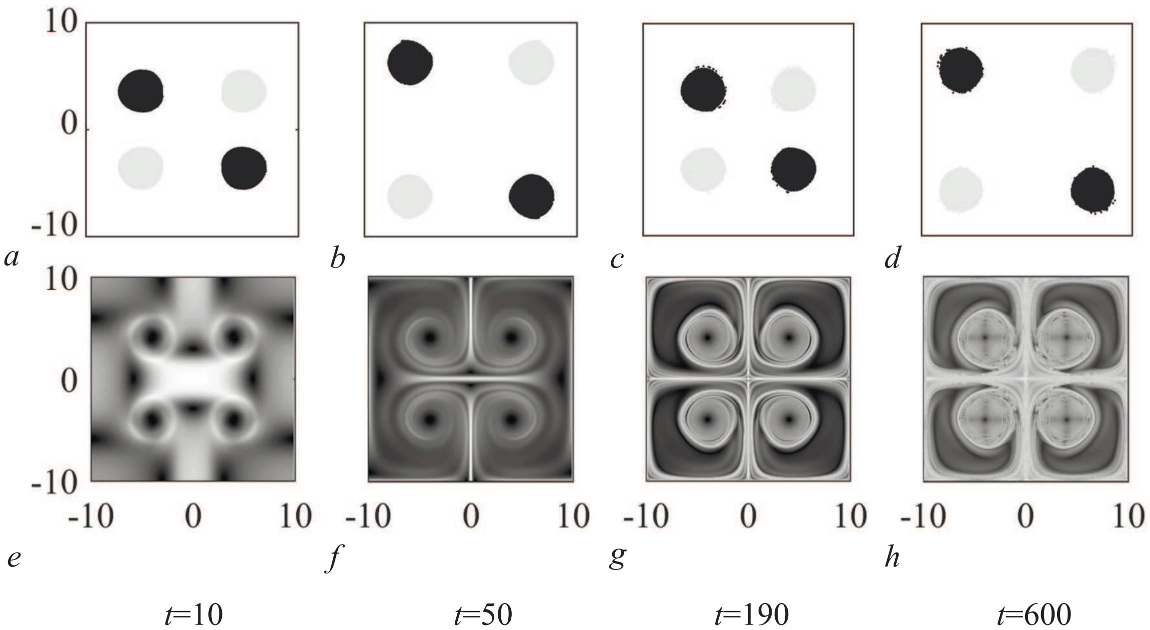

Fig. 2. (a–d) – the vorticity distribution on the (x, y) plane and (e–h) – the Lyapunov exponents at the specific time t for a vortex configuration of four vortices (5) for $R = 2.0$ and $\alpha = \beta = 4.0$

of the computational domain, both dipoles meet structures identical to them, and again a four-patch configuration is formed.

The figure of the LLE field shows that the particles recede much more along the separatrices, with the vertical separatrix $t \approx 50$ being formed first (see Fig. 2,*f*), followed by the horizontal one $t = 190$ (see fig. 2, *g*. The transport of passive particles around the patches is weaker than the transport inside the patches.

In the following two experiments the vorticity distribution, the patch radius $R = 3.5$ and the shift of the patch centers $\alpha = \beta = 5.0$ were identical at the initial time. The only thing to differ was the location of the patches with the total vorticity of different signs.

Fig. 3 shows that at the initial moment of time patches of the same sign are located diagonally, that is, the patches with a total negative vorticity are in the left top and right bottom areas, and the patches with a total positive vorticity are in the top right and bottom left areas. From the very beginning of the calculation, a symmetrical deformation of the patches occurs, which is clearly visible at $t = 15$ (see Fig. 3, *e*). Next, filamentation occurs, which leads to the formation of patches of a new shape. Such a structure is preserved further in time over the entire calculation interval $t \in [65, 400]$, with the whole structure standing still, and each of the patches rotates around its axis, making one complete rotation in $t \approx 10$, which is much faster than in the previous experiment.

As the analysis the LLE field shows, the formation of horizontal and vertical separatrices takes place, as it does in previous experiments. The mixing processes at $t = 65$ are more intense than at $t = 400$. This is due to the fact that at the initial times the structure just starts to form, and then it remains without qualitative changes up to $t = 400$.

Fig. 4 shows that at the initial moment of time, patches of the same sign are located in one column, that is, the patches with a total positive vorticity are in the upper left and lower left areas, the patches with a total negative vorticity are in the upper right and lower right areas. The dynamics of such a structure qualitatively differs from the previous experiment at the initial stage of the calculation. At $t = 10$ (see Fig. 4, *a*), a symmetrical deformation of all patches occurs, which at time $t = 45$

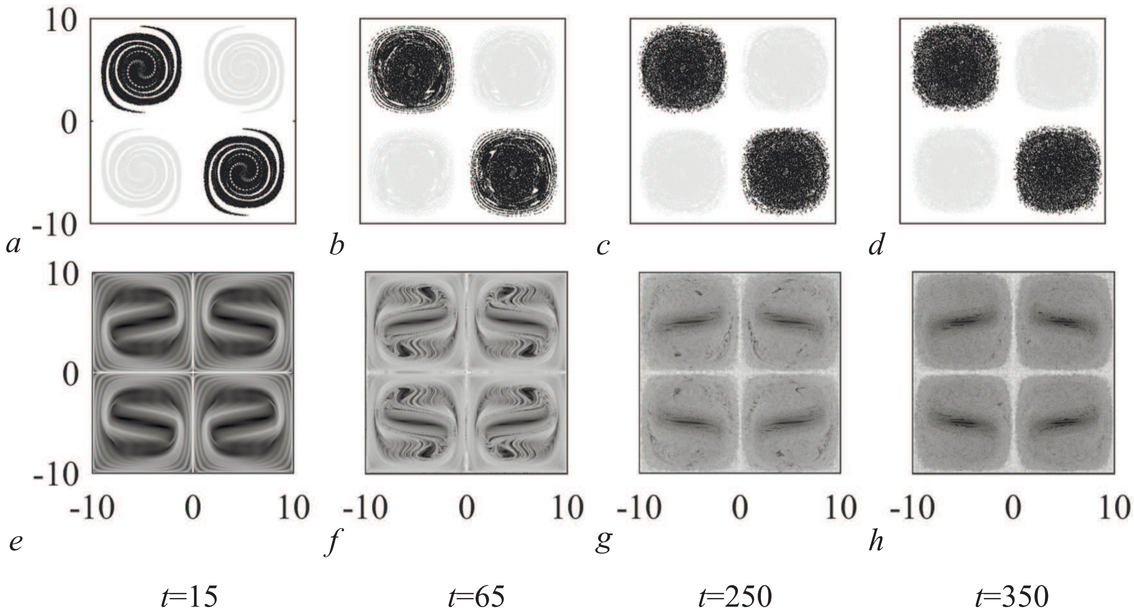

Fig. 3. (*a–d*) – the vorticity distribution on the (x, y) plane and (*e–h*) – the Lyapunov exponents at the specific time t for a vortex configuration of four vortices (5) for $R = 3.5$ and $\alpha = \beta = 5.0$

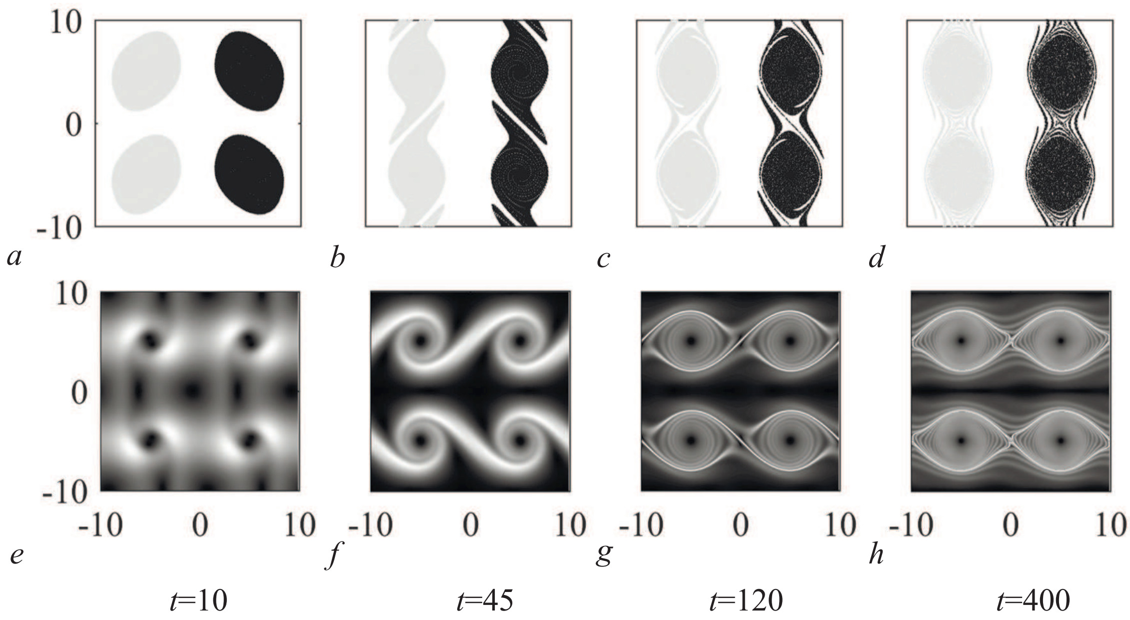

Fig. 4. (*a–d*) – the vorticity distribution on the (x, y) plane and (*e–h*) – the Lyapunov exponents at the specific time t for a vortex configuration of four vortices (5) for $R = 3.5$ and $\alpha = \beta = 5.0$

(see Fig. 4, b) leads to the interaction and mixing of patch particles of the same sign. At the same time, the formation of a new quasistationary structure begins.

By the time instant $t = 120$ (see Fig. 4, c) a symmetrical web-like structure is formed, which is preserved over the entire calculation interval $t \in [120, 400]$.

An analysis of LLE allows us to conclude that the particles are transported in the area: the particles that are most receded are those that are at the initial moment of time at the boundary of each patch. At $t = 45$ (see Fig. 4,f) the recession is stronger than at $t = 400$ (see Fig. 4, h), which indicates the fact that a new quasistationary structure has formed in the liquid. Unlike all previous calculations, the formation of vertical and horizontal separatrices does not occur here.

4. Advection of particles in a liquid

This section presents the results of the analysis of the trajectories of liquid particles on the entire plane for the vortex configurations discussed in the previous section.

Since this problem is considered under periodic boundary conditions, for each particle that left the region during the calculation, it is possible to trace its trajectory on the entire plane. The trajectories of the following particles were studied: vorticity centers of patches, internal particles of patches close to separatrices, random particles. The trajectories of all of them are given and analyzed below.

Fig. 5 shows the particle trajectories corresponding to Fig. 1 and Fig. 2.

Fig. 5, a presents particle trajectories that correspond to the scenario when the parquet structure is preserved for long times. Each of the patches of the vortex parquet stands still and rotates around its axis. This means that the trajectories of their vorticity centers are points. The internal particles of patches of this configuration will rotate in a circle around the center of vorticity at a constant speed. The farther the particle is from the center, the greater the radius of its circular trajectory. Particles lying on the separatrices (or close to them) will recede along the separatrices almost in a straight line. If the particle goes beyond the limits of the computational domain, it continues its motion along the separatrix further on the plane. All these cases are shown in Fig. 5, a for $t \in [0, 400]$.

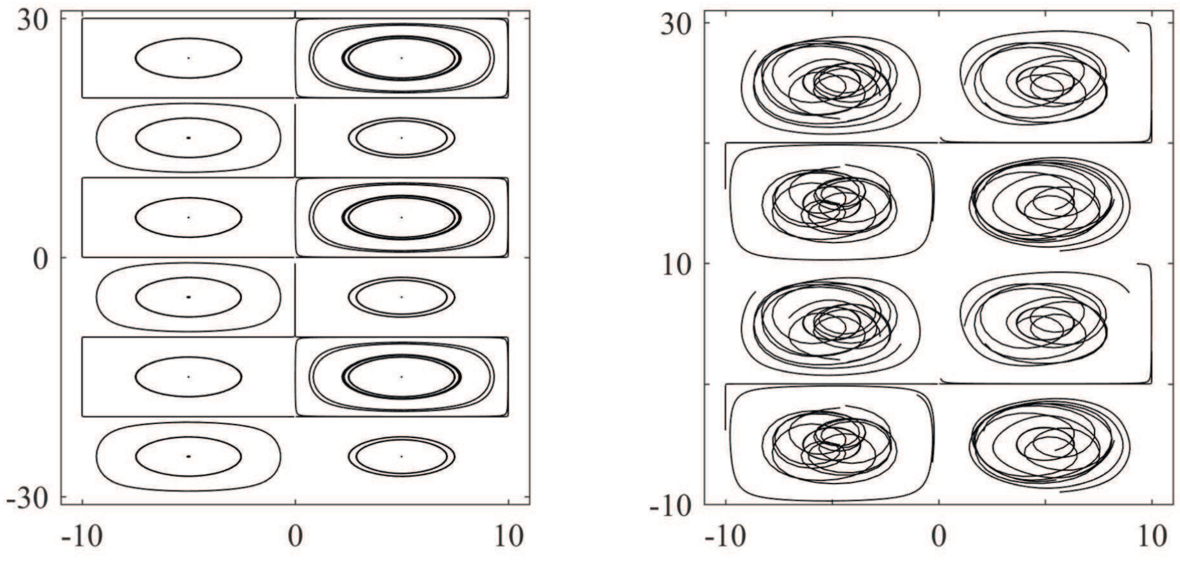

a *b*

Fig. 5. Particle trajectories over the plane for a vortex parquet (5): *a* – with a patch radius $R = 2.5$ and $\alpha = \beta = 5.0$; *b* – with a patch radius $R = 2.0$ and $\alpha = \beta = 4.0$

Fig. 5, *b* presents particle trajectories that correspond to the scenario when periodic motion is observed on the plane. The trajectories of both the vorticity centers and the internal particles of the patches are spirals corresponding to the movement of the patches in Fig. 2, *a*–*d*. Particles close to the separatrices move along them over the entire plane. Due to cumbersomeness, Fig. 5, *b* shows only the trajectories on the interval $t \in [0, 300]$.

Fig. 6 shows the particle trajectories corresponding to Fig. 3 and Fig. 4. Fig. 6, *a* corresponds to the scenario when the patches that make up the vortex parquet are deformed at short times and

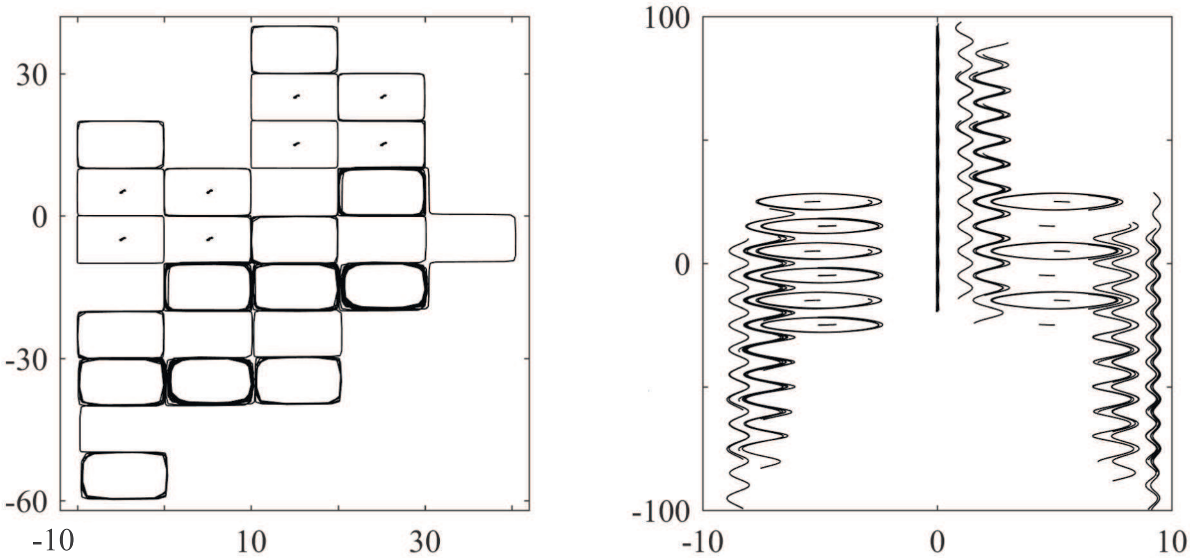

a *b*

Fig. 6. Particle trajectories over the plane for a vortex parquet (5): *a* – with a patch radius $R = 3.5$ and $\alpha = \beta = 5.0$; *b* – with a patch radius $R = 3.5$ and $\alpha = \beta = 5.0$

form a new structure, which is preserved further in time. For particles that are vorticity centers, a slight displacement is observed corresponding to a change in the patch. Particles moving along the separatrices recede over the entire plane, forming a cellular structure similar to the structure of trajectories in the computational domain.

Fig. 6, *b* shows the particle trajectories corresponding to Fig. 4. It can be seen that the particles, which are the centers of vorticity of each of the patches, stand still throughout the computation. The internal particles of the patches rotate around the center of vorticity along a circular trajectory at a constant speed. The boundary particles of the patches move along the entire plane along a sinusoidal trajectory, which corresponds to the scenario of the formation of a quasistationary web structure obtained under the conditions of this computational experiment. For particles lying on the separatrices, the trajectories are straight lines.

Conclusion

The article presents the results of a numerical study of the dynamics of vortex parquet by analyzing the field of local Lyapunov exponents and the trajectories of liquid particles on the plane. A vortex configuration consisting of four patches of the same size located at the nodes of an evenly spaced grid and having different orientations is considered. This configuration is an area of the vortex parquet on the plane. The correlation between the radii and the relative positions of patches of different directions on the one hand and the dynamics and advection in the vortex parquet on the other is studied. The results of a numerical calculation of the dynamics of liquid particles and local Lyapunov exponents at various points in time are presented.

It is shown that in the case of an initial configuration that is symmetrical on the entire plane, the entire structure stands still, while each of the patches rotates around its axis with a constant speed. In the event of symmetry breaking, several scenarios are possible depending on the parameters of the initial distribution: periodic dynamics, the formation of a quasistationary structure, and the formation of a web.

It is detected that with the same initial parameters of the calculation configuration, the mutual arrangement of patches of different directions at the initial moment of time has a significant effect on the dynamics of the entire vortex parquet.

References

1. Grigoryev Yu.N., Vshivkov V.A. Numerical Methods «Particle-in-Cells». Novosibirsk: Nauka, 2000 (in Russian).
2. Dynnikova G.Ya. Fast technique for solving the N-body problem in flow simulation by vortex methods. *Computational Mathematics and Mathematical Physics*, 2009, vol. 49, no. 8, pp. 1389–1396.
3. Cottet G.H., Koumoutsakos P.D. Vortex methods. Cambridge University Press, 2000.
4. Govorukhin V.N. A vortex method for computing two-dimensional inviscid incompressible flows. *Computational Mathematics and Mathematical Physics*, 2011, vol. 51, no. 6, pp. 1061–1073.
5. Govorukhin V.N. Numerical analysis of the dynamics of distributed vortex configurations. *Computational Mathematics and Mathematical Physics*, 2016, vol. 56, no. 8, pp. 1474–1487.
6. Revina S.V. Stability of the Kolmogorov flow and its modifications. *Computational Mathematics and Mathematical Physics*, 2017, vol. 57, no. 6, pp. 995–1012.
7. Fortova S.V., Oparina E.I., Belotserkovskaya M.S. Numerical simulation of the Kolmogorov flow under the influence of the periodic field of the external force. *Journal of Physics: Conference Series*, 2018, vol. 1128, 012089.

8. Dombre T., Frisch U., Greene J.M., Hénon M., Mehr A., Soward A.M. Chaotic Streamlines in the ABC Flows. *Journal of Fluid Mechanics*, 1986, vol. 167, pp. 353–391.
9. Govorukhin V.N., Morgulis A.B.,Yudovich V.I., Zaslavsky G.M. Chaotic advection in compressible helical flow. *Physical review E*, 1999, vol. 60, no. 3.
10. Zaslavskii G.M., Sagdeev R.Z., Usikov D.A., Chernikov A.A. Minimal chaos, stochastic webs, and structures of quasicrystal symmetry. *Sov. Phys. Usp*, 1988, vol. 31, pp. 887–915.
11. Zaslavky G.M. The Physics of Chaos in Hamiltonian Systems. Second edition. Imperial College Press, 2007.
12. Govorukhin V.N., Filimonova A.M. Numerical calculation of planar geophysical flows of an inviscid incompressible fluid by a meshfree-spectral method. *Computer research and modelling*, 2019, vol. 11, no. 3, pp. 413–426 (in Russian).
13. Govorukhin V.N. On the choice of a method for integrating the equations of motion of a set of fluid particles. *Computational Mathematics and Mathematical Physics*, 2014, vol. 54, no. 4, pp. 706–718.
14. Aubry A., Chartier P. Pseudo-symplectic Runge-Kutta methods. *BIT*, 1998, vol. 38, no. 3. pp. 439–461.
15. Shadden S., Lekien F., Marsden J. Definition and properties of Lagrangian coherent structures from finite-time Lyapunov exponents in two-dimensional aperiodic flows. *Phys. D: Nonlinear Phenomena*, 2005, vol. 212, no. 3–4, pp. 271–304.
16. Haller G. Finding finite-time invariant manifolds in two-dimensional velocity fields. *Chaos*, 2000, vol. 10, no. 1, pp. 99–108.